Phospholipid Subclass Specific Alterations in the Passive Ion Permeability of Membrane Bilayers: Separation of Enthalpic and Entropic Contributions to Transbilayer Ion Flux†

Youchun Zeng, Xianlin Han, and Richard W. Gross*

Departments of Internal Medicine, Chemistry, and Molecular Biology & Pharmacology, Division of Bioorganic Chemistry and Molecular Pharmacology, Washington University School of Medicine, St. Louis, Missouri 63110

Received October 10, 1997; Revised Manuscript Received December 12, 1997

ABSTRACT: Alterations in phospholipid class, subclass, and individual molecular species contribute to the diversity of biologic membranes, but their effects on membrane passive ion permeability have not been systematically studied. Herein, we developed a simple and efficient fluorescence technique based upon the loss of valinomycin-inducible membrane potential to characterize the passive flux of ions across phospholipid bilayers. Detailed kinetic characterization of ion flux across membrane bilayers composed of discrete chemical entities demonstrated that the class, subclass, and individual molecular species of each phospholipid have substantive effects on membrane passive ion permeability properties. Increasing the degree of unsaturation in either the *sn*-1 or *sn*-2 aliphatic chains in phosphatidylcholine markedly enhanced transmembrane ion flux, with over 10-fold differences in the first-order rate constant manifested in molecular species containing four double bonds in comparison to those possessing three double bonds (e.g., $k_{app} = 0.0014$ min^{-1} for 1-octadec-9′-enoyl-2-octadec-9′,12′-dienoyl-*sn*-glycero-3-phosphocholine (18:1-18:2 phosphatidylcholine) while $k_{app} = 0.021$ min^{-1} for 1,2-dioctadec-9′,12′-dienoyl-*sn*-glycero-3-phosphocholine (18:2-18:2 phosphatidylcholine)). Moreover, although the apparent first-order rate constants for transmembrane ion flux in vesicles composed of phosphatidylcholine or plasmanylcholine containing palmitate at the *sn*-1 position and arachidonate at the *sn*-2 position were similar ($k_{app} = 0.04$ min^{-1} at 22 °C for both), the k_{app} for corresponding vesicles composed of plasmenylcholine was 20-fold less ($k_{app} = 0.002$ min^{-1} at 22 °C). Examination of the temperature dependence of passive membrane ion permeability demonstrated that altered ion flux across membranes composed of choline glycerophospholipids was primarily due to entropic effects without substantial changes in the activation energy for ion translocation. For example, $E_a = 19.7 \pm 0.5$ and 20.7 ± 0.6 kcal·mol^{-1} for 1-hexadecanoyl-2-eicosa-5′,8′,11′,14′-tetraenoyl-*sn*-glycero-3-phosphocholine (16:0-20:4 phosphatidylcholine) and 1-*O*-*(Z)*-hexadec-1′-enyl-2-eicosa-5′,8′,11′,14′-tetraenoyl-*sn*-glycero-3-phosphocholine (16:0-20:4 plasmenylcholine), respectively, while their difference in the entropies of activation (ΔS) was 4.3 ± 0.5 cal·mol^{-1}·K^{-1}. Collectively, these results identify substantial differences in the membrane passive ion permeability properties of phospholipid classes, subclasses, and molecular species present in biologic membranes of eukaryotic cells and identify entropic alterations as an important contributor to these differences.

Biologic membranes are organized assemblies of phospholipids, proteins, and cholesterol that provide the structural framework for a wide variety of membrane functions including (1) a membrane permeability barrier (*1*, *2*), (2) an appropriate environment for the optimal function of transmembrane proteins such as ion channels and ion pumps (*3*−*5*), and (3) an interfacial matrix that facilitates the stereoselective interactions of a wide variety of cellular hydrophobic and hydrophilic constituents (*6*, *7*). By far, phospholipids comprise the predominant chemical components present in biologic membranes and their precise chemical composition is specifically tailored to individual subcellular membrane functions through utilization of a wide diversity of covalent alterations in phospholipid molecular structure (*8*, *9*). The covalent diversity in phospholipid structure is manifest by alterations in the polar headgroup (e.g., choline, serine, or ethanolamine leading to phospholipid class diversity), the covalent linkage at the *sn*-1 position (e.g., ester, ether, or vinyl ether leading to phospholipid subclass diversity), or the nature of the aliphatic chains (leading to individual molecular species diversity). It is a fundamental tenet of membrane chemistry that this diversity in phospholipid covalent structures is an important determinant of membrane function (*10*, *11*). Although the role of this covalent diversity in transmembrane protein function and intermolecular in-

† This research was supported jointly by grants from the Juvenile Diabetes Foundation International File # 996003 and NIH grants 1 PO1 HL 57278-02 and 2 R01 HL 41250-06A1.

* To whom correspondence should be addressed at the Washington University School of Medicine, Division of Bioorganic Chemistry and Molecular Pharmacology, 660 South Euclid Avenue, Campus Box 8020, St. Louis, MO 63110. Telephone number: 314-362-2690. Fax number: 314-362-1402.

S0006-2960(97)02517-8 CCC: $15.00
Published on Web 02/05/1998

teractions has been intensely studied (*8*, *9*, *12*, *13*), the role of these different structural alterations on the passive ion permeability properties of biologic membranes has not been examined in systematic detail.

In most cell types, biologic membranes are composed predominantly of diacyl phospholipid molecular species. However, plasmalogen molecular species are the predominant phospholipid subclass present in many electrically active membranes (*14*−*16*). Indeed, in two specialized electrically active membrane systems in muscle, sarcolemma and sarcoplasmic reticulum, plasmalogen molecular species actually constitute the major phospholipid subclass (*14*, *15*). Recent studies have identified the importance of plasmalogen molecular species in modulating the kinetic properties of ion channels (e.g., gramicidin) and ion carriers (e.g., valinomycin) (*4*, *5*). While the importance of ion channels and ion transporters in mediating cellular electrophysiologic characteristics is clear and undisputed, it is important to recognize that transmembrane ion gradients are also influenced by the passive membrane permeability properties of biologic membranes in electrically active tissues (*17*−*21*). Due to the technical difficulties inherent in the direct measurement of the passive membrane permeability of lipid vesicles, the roles of phospholipid classes, subclasses, and individual molecular species in modulating the electrical properties of biologic membranes have not been fully elucidated. Herein, we describe a simple and rapid fluorescence technique suitable for the direct measurement of passive membrane permeability of a wide variety of phospholipid bilayers and utilize this methodology to systematically characterize alterations in the passive ion permeability properties of membranes composed of distinct phospholipid classes, subclasses, and individual molecular species. The results demonstrate that membranes composed of plasmenylcholine are much less permeable than those composed of either phosphatidylcholine or plasmanylcholine, that vesicles composed of phosphatidylserine leak ions at rates substantially lower than vesicles composed of phosphatidylcholine, and that increasing the degree of olefin centers in the aliphatic chain of each phospholipid class increases transmembrane passive ion permeability. Moreover, we show that entropic alterations are the principal determinant of passive ion translocation among phospholipids containing similar surface charge distributions.

MATERIALS AND METHODS

Materials. Lysoplasmenylcholine and plasmenylcholine were synthesized from bovine heart lecithin, as described previously (*22*). Other phospholipids were purchased from Avanti Polar Lipids, Inc. (Alabaster, AL). All choline glycerophospholipids were further purified by reversed-phase HPLC and extracted twice with the Bligh and Dyer procedure (*23*). The phospholipid concentrations were determined by capillary gas chromatography after acid methanolysis utilizing arachidic acid (20:0) as an internal standard (*24*). 3,3′-Dipropylthiadicarbocyanine iodide ($diSC_3(5)$)[1] was supplied by Molecular Probes, Inc. (Eugene, OR). Cholesterol was purchased from Nu Chek Prep, Inc. (Elysian, MN). Most other chemicals were obtained from Sigma Chemical Co. (St. Louis, MO).

Preparation of Small Unilamellar Vesicles. Phospholipids or their binary mixtures with cholesterol (2 μmol in total) were dissolved in chloroform, dried under a nitrogen stream, and subsequently subjected to high vacuum (less than 50 mTorr) for at least 2 h. The dried lipid film was suspended in 0.6 mL of buffer A (0.29 M K_2SO_4, pH = 6.3) by vigorous vortexing for 2 min and subsequent sonication (4 min, 40% duty cycle) twice utilizing a Vibra Cell Model VC 600 sonicator (Sonics Material, Danbury, CT) under a nitrogen atmosphere. The average diameter of the vesicles, as measured by the light-scattering method (*25*) with a submicron particle analyzer (Coulter, Hialeah, FL), was about 30 nm, which was consistent with our previous results utilizing inulin trapping (*26*).

Measurement of Passive Membrane Permeability. Sealed vesicles in buffer A were diluted 100-fold with a K^+ free isoosmotic buffer B (0.29 M Li_2SO_4, pH = 6.3) to create an ion concentration gradient by addition of 20 μL of vesicles in buffer A to 2.0 mL of buffer B with stirring (Scheme 1, step 1). Next, the diluted vesicles were gently stirred for up to 3 days at 22 °C. Passive ion leakage resulted in a change in the ion concentration gradient across the membrane (Scheme 1, step 2), which was quantified utilizing a potential-sensitive dye ($diSC_3(5)$) after a valinomycin-induced transmembrane potential was generated. Briefly, the fluorescence intensities of $diSC_3(5)$ (*27*) were measured with a SLM 4800C spectrofluorometer (SLM Instrument, Urbana, IL) employing an excitation wavelength of 618 nm (8 nm slit width) through a monochromator and an emission wavelength of 690 nm (8 nm slit width) through a monochromator. After the diluted vesicle solution had been gently stirred for selected time intervals, 4 μL of $diSC_3(5)$ solution (0.27 mg/mL in ethanol) was added with a Hamilton microliter syringe directly to the vesicle solution (final $diSC_3(5)$ concentration 1 μM) and then fluorescence intensity was recorded as a function of time (Scheme 1, step 3). Next, 4 μL of valinomycin solution (0.56 mg/mL in ethanol, final valinomycin concentration 1 μM) was added with a Hamilton microliter syringe to generate a transmembrane potential. The passive ion leakage at each time interval (t) can be monitored by the determination of the magnitude of the transmembrane potential created after the addition of valinomycin (Scheme 1, step 4).

Data Analysis. In the limiting case, where the valinomycin-facilitated potassium ion permeability strongly predominates (in comparison to other ions), the transmembrane potential is equal and opposite to the chemical potential of potassium ions, due only to the transmembrane concentration

[1] Abbreviations: 16:0-18:1 phosphatidylcholine, 1-hexadecanoyl-2-octadec-9′-enoyl-*sn*-glycero-3-phosphocholine; 16:0-18:1 phosphatidylethanolamine, 1-hexadecanoyl-2-octadec-9′-enoyl-*sn*-glycero-3-phosphoethanolamine; 16:0-18:1 phosphatidylserine, 1-hexadecanoyl-2-octadec-9′-enoyl-*sn*-glycero-3-phosphoserine; 16:0-20:4 phosphatidylcholine, 1-hexadecanoyl-2-eicosa-5′,8′,11′,14′-tetraenoyl-*sn*-glycero-3-phosphocholine; 16:0-20:4 phosphatidylserine, 1-hexadecanoyl-2-eicosa-5′,8′,11′,14′-tetraenoyl-*sn*-glycero-3-phosphoserine; 16:0-20:4 plasmanylcholine, 1-*O*-hexadecyl-2-eicosa-5′,8′,11′,14′-tetraenoyl-*sn*-glycero-3-phosphocholine; 16:0-20:4 plasmenylcholine, 1-*O-(Z)*-hexadec-1′-enyl-2-eicosa-5′,8′,11′,14′-tetraenoyl-*sn*-glycero-3-phosphocholine; 18:1-18:1 phosphatidylcholine, 1,2-dioctadec-9′-enoyl-*sn*-glycero-3-phosphocholine; 18:1-18:2 phosphatidylcholine, 1-octadec-9′-enoyl-2-octadec-9′,12′-dienoyl-*sn*-glycero-3-phosphocholine; 18:2-18:2 phosphatidylcholine, 1,2-dioctadec-9′,12′-dienoyl-*sn*-glycero-3-phosphocholine; 18:3-18:3 phosphatidylcholine, 1,2-dioctadec-9′,12′,15′-trienoyl-*sn*-glycero-3-phosphocholine; $diSC_3(5)$, 3,3′-dipropylthiadicarbocyanine iodide; PC, phosphatidylcholine; PS, phosphatidylserine.

Scheme 1: Flow Chart for Measurements of Passive Ion Permeability of Phospholipid Vesicles[a]

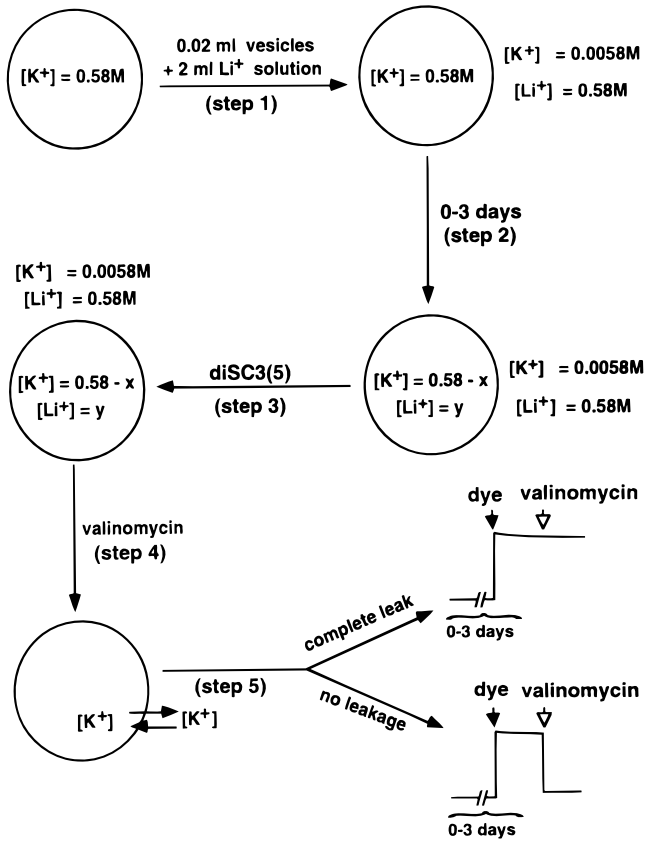

[a] Small unilamellar vesicles were prepared in K^+ medium (0.29 M K_2SO_4, pH 6.3 at 22 °C) and were diluted 100-fold with isoosmotic Li^+ medium (0.29 M Li_2SO_4, pH 6.3 at 22 °C) as described in the Materials and Methods. This resulted in the generation of a chemical potential across the bilayer membrane (step 1). Next, the diluted vesicles were gently stirred for 0−3 days at 22 °C (step 2) prior to addition of the potential-sensitive fluorescence dye, $diSC_3(5)$ (final concentration, 1×10^{-6} M, dissolved in 4 μL of ethanol). The chemical potential was transduced into an electrical potential by the addition of the K^+ ionophore valinomycin (final concentration, 1×10^{-6} M, dissolved in 4 μL of ethanol) (steps 3 and step 4). The fluorescence emission of the potential-sensitive dye was monitored at 690 nm after excitation at 618 nm (step 5). "X" = the loss of the concentration of K^+ inside the vesicle; "Y" = the concentration of Li^+ inside the vesicle. "-//-" indicates the aging time of the vesicles; "↓" represents the addition of $diSC_3(5)$ as in step 3; the open downward arrow represents the addition of valinomycin as in step 4.

gradient of K^+ across the vesicle membrane, and can be calculated by the Nernst equation:

$$\Delta U = (RT/F)\ln([K^+]_{out}/[K^+]_{in}) \quad (1)$$

where ΔU is the transmembrane potential, R is the ideal gas constant (8.314 J·mol^{-1} K^{-1}), F is Faraday's constant (96 500 C·mol^{-1}), $[K^+]_{out}$ and $[K^+]_{in}$ are the concentrations of potassium ions outside and inside the vesicle, respectively. In this study, the initial transmembrane potential (ΔU) was 0.118 V utilizing the initial concentration gradients employed.

For subsequent calculations we have assumed that these unilamellar vesicles have a diameter of approximately 30 nm (*26*) and possess a membrane thickness of approximately 4 nm, with a dielectric constant in the membrane interior ≈2 (*8*). The membrane bilayer of a vesicle can be treated as a spherical electric capacitor (*8*). For the first-order approximation, we assume that all the net charges are on either the interior or the exterior surface of the vesicle membranes. According to Gauss's law, the electric field between the interior and exterior surface of the vesicle bilayer is

$$E = -Q/(4\pi\epsilon_o\epsilon_r r^2) \quad (2)$$

where Q is the charge on either the interior or exterior surface of the vesicle bilayer, r is the radius, ϵ_o is the absolute vacuum permittivity (8.85×10^{-12} C^2·m^{-2}·N^{-1}), and ϵ_r is the dielectric constant of the membrane bilayer. The transmembrane potential is given by

$$\Delta U = U_{ex} - U_{in} = \int_{r_{in}}^{r_{ex}} E\,dr = Q(1/r_{in} - 1/r_{ex})/(4\pi\epsilon_o\epsilon_r) \quad (3)$$

where r_{in} is the radius of the interior surface of the vesicle membrane (11 nm) and r_{ex} is the radius of the exterior surface of the vesicle membrane (15 nm). The electric capacitance of a vesicle is

$$C_v = Q/\Delta U = 4\pi\epsilon_o\epsilon_r/(1/r_{in} - 1/r_{ex}) \approx 9.2 \times 10^{-18} F \quad (4)$$

Since the unitary charge of a potassium ion is 1.6×10^{-19} C, then the number of potassium ions that can diffuse out of the vesicle to result in a transmembrane potential of 0.118 V is given by

$$N = Q/1.6 \times 10^{-19} = 4\pi\epsilon_o\epsilon_r\Delta U/(1/r_{in} - 1/r_{ex})/1.6 \times 10^{-19} \approx 7 \quad (5)$$

Furthermore, the trapped aqueous volume within a 30 nm vesicle is

$$V_{in} = (4\pi/3) \times r_{in}{}^3 = (4\pi/3)11^3 \approx 5572\ \text{nm}^3 \quad (6)$$

In these experiments, the initial concentration of K^+ is 0.58 M, and the total number of K^+ trapped within a vesicle is

$$N_{total} = 6.02 \times 10^{23} \times 0.58 V_{in} \approx 1946 \quad (7)$$

Thus the number of K^+ ions that diffuse out of a vesicle to promote a transmembrane potential of 0.118 V is approximately 0.4% of the total K^+ content trapped within the vesicle. Since the anionic counter currents are negligible with SO_4^{2-} buffer, subsequent K^+ efflux will occur only as Li^+ ions permeate into the vesicle.

From the time-course experiments and an experimentally derived calibration curve of fluorescence intensity and transmembrane potential, we can compute the rate of the decrease in the concentration of the potassium ions inside the vesicles ($-d[K^+]_{in}/dt$). If the passive ion permeability is first order with respect to the ion concentration, the rate law for the leakage of potassium ions is

$$-d[K^+]_{in}/dt = k[K^+]_{in} \quad \text{or} \quad \ln[K^+]_{in} = -kt + C \quad (8)$$

where $[K^+]_{in}$ is the concentration of the potassium ions inside the vesicles, t is time, and C is an integration constant. The specific rate constant, k, can be calculated from the rate of leakage of the potassium ions from inside the vesicles.

Table 1: Effects of Acyl Chain Composition on Passive Ion Permeability

phosphatidylcholine[a]	rate constant[b] (1/min)	rate of K^+/Li^+exchange[c] [(1/min)/vesicle]
18:1-18:1	<0.0001	<0.2
18:1-18:2	0.0014	3
18:2-18:2	0.021	41
18:3-18:3	≫1	>1000

[a] 18:*n*-18:*m* phosphatidylcholine, *n* is the number of double bonds in the *sn*-1 acyl chain; *m* is the number of double bonds in the *sn*-2 acyl chain. [b] Passive ion permeability was measured as described in the legend of Figure 5. The rate constants were calculated from the slope of the initial loss of chemical potential as described in the Materials and Methods. [c] The rates of ion flux were calculated from the trapped volume and the initial rate of change in the potassium ion concentration, assuming the vesicle has a diameter of 30 nm as described in the Materials and Methods.

Table 2: Effects of Cholesterol on Passive Ion Permeability in Bilayers Composed of 16:0-20:4 Phosphatidylcholine[a]

cholesterol (mol %)	rate constant (1/min)	rate of K^+/Li^+exchange[b] [(1/min)/vesicle]
0	0.04	78
15	0.016	31
30	0.009	17

[a] Passive ion permeability was measured as described in the legend of Figure 6. The rate constants were calculated from the slope of the initial loss of chemical potential as described in the Materials and Methods. [b] The rates of ion flux were calculated from the trapped volume and the initial rate of change in the potassium ion concentration, assuming the vesicle has a diameter of 30 nm as described in the Materials and Methods.

For the first-order approximation, we assume the probability factor (A) is identical for all phospholipids with similar surface charge distributions, the apparent activation energy and entropy of the passive ion permeability, E_a and S_a, can be calculated by using the equation

$$k = Ae^{S_a/R}e^{-E_a/RT} \quad \text{or} \quad \ln k = \ln A + S_a/R - E_a/RT \tag{9}$$

where k is the rate constant of the membrane passive ion flux, A is a probability factor, R is the ideal gas constant (8.314 J·mol^{-1}·K^{-1}), and T is the absolute temperature. Activation entropies (S_a) of other phospholipids were calculated relative to the activation entropy of 16:0-20:4 phosphatidylcholine, which had been defined as S'. Similarly, the relative free energies of activation at 295 K were computed relative to that of 16:0-20:4 phosphatidylcholine, (defined as G'), assuming the activation energies for each phospholipid are identical within experimental error, which was shown experimentally in Table 3. The rate of potassium ion efflux per vesicle can be calculated from the trapped aqueous volume and the change in the potassium ion concentration inside the vesicle:

$$dN/dt = -6.02 \times 10^{23} V_{in}(d[K^+]_{in}/dt) \tag{10}$$

where V_{in} is the trapped aqueous volume per vesicle.

RESULTS

Passive Ion Permeability of Vesicles Composed of Different Phospholipid Classes. Membrane vesicles composed of 1-hexadecanoyl-2-octadec-9′-enoyl-*sn*-glycero-3-phosphocholine (16:0-18:1 phosphatidylcholine) maintained an ion concentration gradient and did not leak captured potassium ions even after 3 days of incubation at 22 °C (Figure 1A). Similarly, vesicles composed of 1-hexadecanoyl-2-octadec-9′-enoyl-*sn*-glycero-3-phosphoserine (16:0-18:1 phosphatidylserine) did not leak entrapped potassium ions (Figure 1B). Additional experiments were attempted with sonicated dispersions of ethanolamine glycerophospholipids. However, sonication of suspensions of 1-hexadecanoyl-2-octadec-9′-enoyl-*sn*-glycero-3-phosphoethanolamine (16:0-18:1 phosphatidylethanolamine) did not form stable vesicles between 28 and 37 °C (the gel−liquid crystal phase transition temperature and the bilayer to hexagonal phase transition temperature for 16:0-18:1 phosphatidylethanolamine are 25 and 71 °C, respectively). Accordingly, to examine the effects of ethanolamine glycerophospholipids, binary dispersions composed predominantly of ethanolamine glycerophospholipid with small amounts of choline glycerophospholipids were investigated. Vesicles composed of up to 85% 16:0-18:1 phosphatidylethanolamine with 16:0-18:1 phosphatidylcholine maintained their intrinsic K^+ concentration gradient for at least 24 h.

The effects of individual molecular species on membrane passive permeability properties were next examined. Remarkably, vesicles composed of phosphatidylcholine containing arachidonic acid at the *sn*-2 position (1-hexadecanoyl-2-eicosa-5′,8′,11′,14′-tetraenoyl-*sn*-glycero-3-phosphocholine (16:0-20:4 phosphatidylcholine)) allowed the rapid passage of potassium ions along their concentration gradient during a 1 h incubation (Figure 1C). The observed K^+ leakage reflects the combined rates of K^+ and Li^+ exchange, since no leakage was manifested utilizing Mg^{2+} as the counterion in the dilution buffer. Accordingly, all measured rates reflect the exchange rate of K^+ and Li^+ passive transmembrane ion movement. In contrast, vesicles composed of arachidonate-containing phosphatidylserine (1-hexadecanoyl-2-eicosa-5′,8′,11′,14′-tetraenoyl-*sn*-glycero-3-phosphoserine (16:0-20:4 phosphatidylserine)) retained the trapped potassium ions even after intervals as long as 2 h

Table 3: Relative Entropy, Energy, and Free Energy of Activation of Passive Ion Permeability in Phospholipid Bilayers[a]

phospholipid	activation entropy[b]/ [(cal/mol)/K]	activation energy (kcal/mol)	free energy[c] (kcal/mol)
16:0-20:4 phosphatidylcholine	S'	19.7 ± 0.5	G'
18:2-18:2 phosphatidylcholine	$S' - 1.3 \pm 0.2$	20.6 ± 0.6	$G' + 0.38 \pm 0.06$
18:1-18:2 phosphatidylcholine	$S' - 5.9 \pm 0.4$	20.9 ± 0.6	$G' + 1.7 \pm 0.1$
16:0-20:4 plasmenylcholine	$S' - 4.3 \pm 0.4$	20.7 ± 0.8	$G' + 1.3 \pm 0.1$

[a] Passive ion permeability was measured as described in the legend of Figure 7. Activation energies and activation entropies were obtained from Arrhennius analysis. Values shown represent the mean ± SD of three independent experiments. [b] Activation entropies of all other phospholipids were calculated relative to the activation entropy of 16:0-20:4 phosphatidylcholine, which has been defined as S'; in addition, the assumption has been made that the probability factors, A, in eq 9, are identical for each phospholipid. [c] Free energies of activation at 295 K were computed relative to the free energy of activation of 16:0-20:4 phosphatidylcholine, which has been defined as G', assuming the activation energies for each phospholipid are identical within experimental error, as shown here.

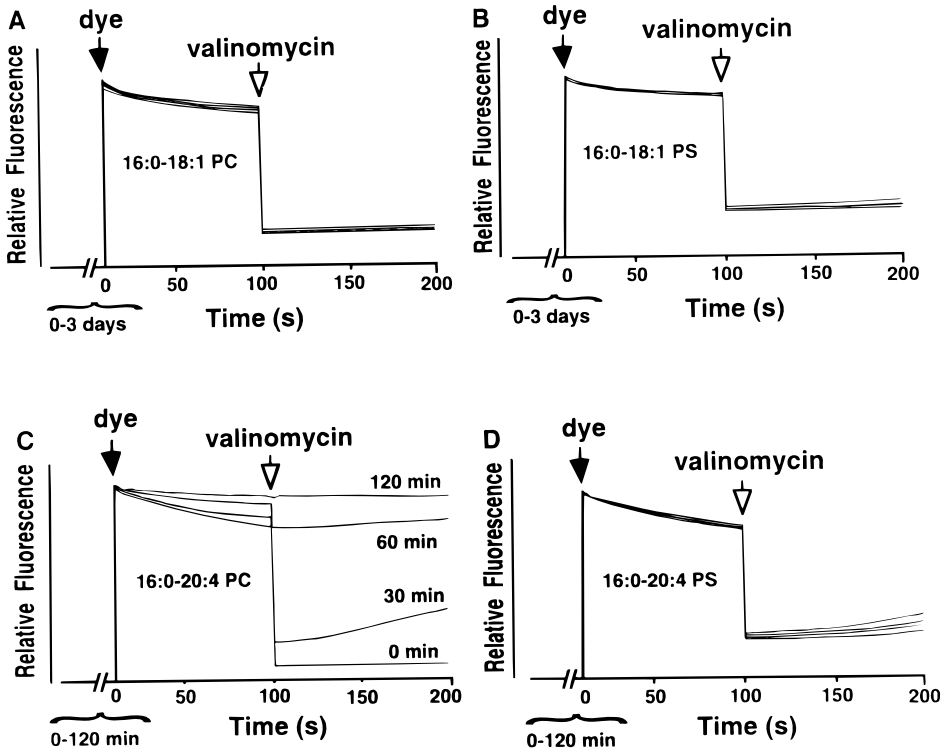

FIGURE 1: Passive ion permeability across phospholipid bilayers. Small unilamellar vesicles ($d \approx 30$ nm) composed of 16:0-18:1 phosphatidylcholine (A), 16:0-18:1 phosphatidylserine (B), 16:0-20:4 phosphatidylcholine (C), or 16:0-20:4 phosphatidylserine (D) were prepared in K^+ medium (0.29 M K_2SO_4, pH 6.3 at 22 °C) as described in the Materials and Methods. Vesicles were diluted 100-fold with isoosmotic Li^+ medium (0.29 M Li_2SO_4, pH 6.3 at 22 °C), resulting in the generation of a chemical potential across the bilayers. The diluted vesicles were gently stirred for zero to 3 days at 22 °C for (A) and (B) or for 0−2 h for (C) and (D) prior to introduction of the potential-sensitive fluorescence dye, $diSC_3(5)$ (final concentration, 1×10^{-6} M, dissolved in 4 μL of ethanol). The chemical potential at the end of the incubation interval was transduced into an electrical potential by the addition of valinomycin (final concentration, 1×10^{-6} M, dissolved in 4 μL of ethanol), and the resultant changes in fluorescence emission were monitored at 690 nm after excitation at 618 nm.

(Figure 1D). To examine the effects of binary dispersions of choline and serine glycerophospholipids containing arachidonate at the *sn*-2 position, vesicles composed predominantly of 16:0-20:4 phosphatidylcholine containing 0−10% 16:0-20:4 phosphatidylserine were prepared. The presence of small amounts of 16:0-20:4 phosphatidylserine significantly attenuated passive ion flux across the membrane bilayer in a concentration-dependent manner (Figure 2). For example, introduction of 10 mol % of 16:0-20:4 phosphatidylserine into a 16:0-20:4 phosphatidylcholine membrane decreased the rate constant of the passive ion permeability from 0.04 to 0.01 min^{-1}. Collectively, these results demonstrate the ability of 16:0-18:1 phosphatidylcholine, 16:0-18:1 phosphatidylserine, and predominantly 16:0-18:1 phosphatidylethanolamine-containing vesicles to maintain K^+ ion gradients for at least 24 h, as well as the importance of the individual molecular species of choline glycerophospholipids (but not serine glycerophospholipids) in determining the passive membrane ion permeability of the bilayer system under study.

Passive Ion Permeability of Membrane Vesicles Composed of Distinct Choline Glycerophospholipid Subclasses. To identify the potential importance of phospholipid subclasses as determinants of the rate of passive ion flux through membrane bilayers, vesicles composed of each choline glycerophospholipid subclass containing arachidonic acid at the *sn*-2 position were prepared. A K^+ concentration gradient was generated by dilution of vesicles containing entrapped K^+ into a lithium sulfate buffer as described in the Materials and Methods. Both diacylcholine glycerophospholipid (i.e., phosphatidylcholine) and alkyl ether choline glycerophospholipid (i.e., plasmanylcholine) containing arachidonic acid at the *sn*-2 position rapidly lost K^+ ions from their intravesicular space, and their rates of K^+ efflux from membrane bilayers composed of these two phospholipid subclasses were similar (Figure 3A,B). In stark contrast, vesicles composed of plasmenylcholine containing arachidonic acid at the *sn*-2 position did not leak K^+ ions substantially even after 2 h and only modestly after 6 h (Figure 3C). The rate of K^+ efflux can be calculated from the rate of loss of the valinomycin-induced potential and the known internal aqueous volumes of the membrane vesicles (Figures 3 and 4). A semilog plot of the rate of loss of K^+ ion from the vesicles composed of diacyl and alkyl ether choline phospholipids was linear as a function of time with a rate constant of 0.04 min^{-1}. The rate of efflux of K^+ ions from arachidonate-containing plasmenylcholine vesicles was first order and had a rate constant 20-fold lower than its corresponding choline glycerophospholipid subclasses (i.e., $k_{app} = 0.002$ min^{-1} for plasmenylcholine containing arachidonic acid at the *sn*-2 position) (Figures 3 and 4).

Effect of Acyl Chain Unsaturation on Passive Ion Permeability of Vesicles Composed of Phosphatidylcholine. The importance of acyl chain unsaturation in the *sn*-1 and *sn*-2 positions was examined by preparing vesicles composed of phosphatidylcholine containing 18-carbon fatty acids differing in their degree of unsaturation. The rate of K^+ efflux from phosphatidylcholine vesicles increased as the degree of unsaturation in the *sn*-1 and *sn*-2 chains increased (Figure 5). The rate of efflux from each type of these vesicles was calculated from analysis of the semilog plot of ion efflux.

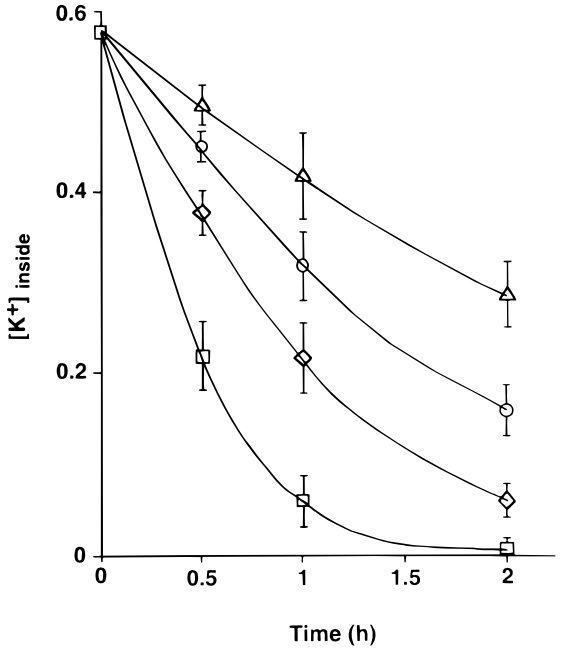

FIGURE 2: Attenuation of ion leakage in vesicles composed of 16:0-20:4 phosphatidylcholine by 16:0-20:4 phosphatidylserine. Small unilamellar vesicles composed of binary mixture of 16:0-20:4 phosphatidylcholine containing 0 mol % (□), 2 mol % (◇), 5 mol % (○), or 10 mol % (△) 16:0-20:4 phosphatidylserine were prepared in K^+ medium (0.29 M K_2SO_4, pH 6.3 at 22 °C) as described in the Materials and Methods. Vesicles were diluted 100-fold with isoosmotic Li^+ medium (0.29 M Li_2SO_4, pH 6.3 at 22 °C), resulting in a chemical potential across the bilayers. The diluted vesicles were gently stirred for 0−120 min at 22 °C prior to addition of the potential-sensitive fluorescence dye, $diSC_3(5)$ (final concentration, 1×10^{-6} M, dissolved in 4 μL of ethanol), and subsequent addition of valinomycin (final concentration, 1×10^{-6} M, dissolved in 4 μL of ethanol). Fluorescence emission was monitored at 690 nm after excitation at 618 nm. The concentrations of K^+ inside the vesicles is calculated from the change in the chemical potential across the vesicular bilayers during the time-course experiment. Data shown represent the means ± SD of three independent experiments.

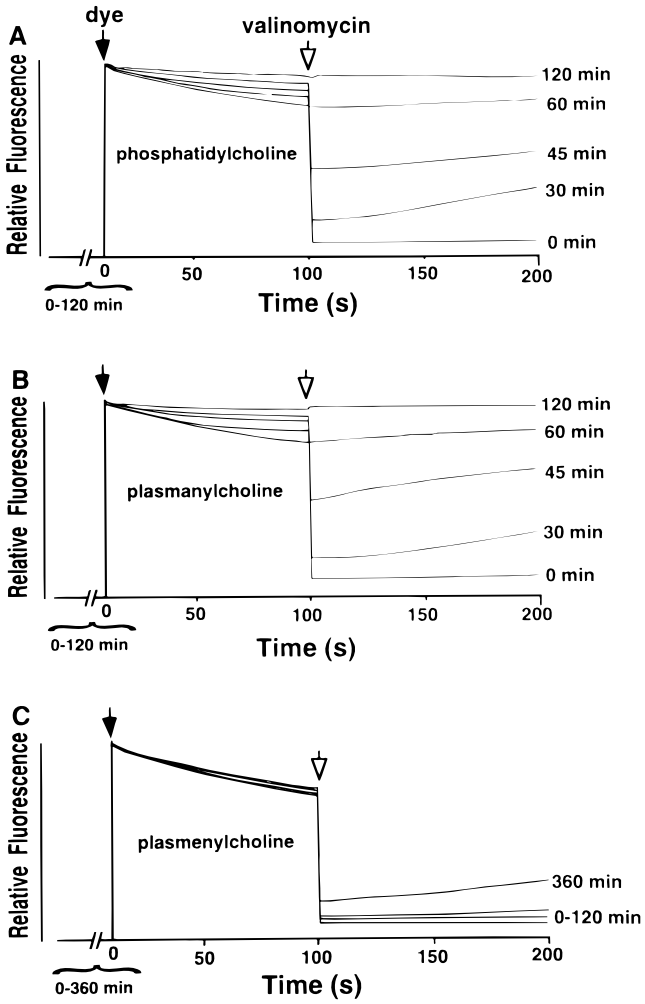

FIGURE 3: Alterations in passive ion permeability of vesicle membranes composed of distinct choline glycerophospholipid subclasses. Small unilamellar vesicles composed of either 16:0-20:4 phosphatidylcholine (A), 16:0-20:4 plasmanylcholine (1-*O*-hexadecyl-2-eicosa-5′,8′,11′,14′-tetraenoyl-*sn*-glycero-3-phosphocholine) (B), or 16:0-20:4 plasmenylcholine (C) were prepared in K^+ medium (0.29 M K_2SO_4, pH 6.3 at 22 °C) as described in the Materials and Methods. Vesicles were diluted 100-fold with isoosmotic Li^+ medium (0.29 M Li_2SO_4, pH 6.3 at 22 °C), resulting in a chemical potential across the bilayers. Next, the diluted vesicles were gently stirred for the indicated times at 22 °C prior to addition of the potential-sensitive fluorescence dye, $diSC_3(5)$ (final concentration, 1×10^{-6} M, dissolved in 4 μL of ethanol). After addition of valinomycin (final concentration, 1×10^{-6} M, dissolved in 4 μL of ethanol), fluorescence emission was monitored at 690 nm with excitation at 618 nm.

These analyses demonstrate that addition of olefin centers results in a dramatic increase in the rate of K^+ efflux (Table 1). Specifically, although no measurable ion efflux is present in vesicles composed of 18:1-18:1 phosphatidylcholine, the rate constants of K^+ efflux in vesicles composed of 18:1-18:2 phosphatidylcholine and 18:2-18:2 phosphatidylcholine were 0.0014 and 0.021 min^{-1}, respectively. The passive efflux of K^+ from 18:3-18:3 phosphatidylcholine vesicles was too rapid to be accurately measured at the temperatures studied.

Effect of Cholesterol on the Passive Membrane Permeability of Vesicles Composed of Choline Glycerophospholipids. Since the plasma membranes of most cells contain substantial amounts of cholesterol, and cholesterol is known to affect membrane permeability (*28*−*31*), detailed studies on the rate of K^+ efflux from vesicles composed of 16:0-20:4 phosphatidylcholine containing selected amounts of cholesterol were performed. Increasing the mole fraction of cholesterol in the membrane bilayer attenuated the rate of K^+ efflux from arachidonate-containing phosphatidylcholine vesicles (Figure 6). For example, in vesicles containing 30 mol % cholesterol, the rate constant of ion efflux decreased to 0.009 min^{-1} from a rate constant of 0.04 min^{-1}, manifested in vesicles without cholesterol (Table 2).

Determination of the Apparent Activation Energy for Passive Ion Flux through Phosphatidylcholine Vesicular Membranes. To determine the apparent activation energy of K^+ efflux and to compare enthalpic and entropic contributions among vesicles composed of individual molecular species and subclasses of choline glycerophospholipids, Arrhenius analysis was performed. Increasing the temperature of vesicles composed of 18:2-18:2 phosphatidylcholine from 4 to 37 °C resulted in an increase in K^+ efflux (Figure 7). Arrhenius analysis of the temperature dependence of K^+ efflux showed a linear slope corresponding to an apparent activation energy $E_a = 21$ kcal/mol. Similarly, K^+ ion efflux increased for 16:0-20:4 phosphatidylcholine, 18:1-18:2 phosphatidylcholine, or 16:0-20:4 plasmenylcholine as a function of temperature. The results demonstrated that activation of

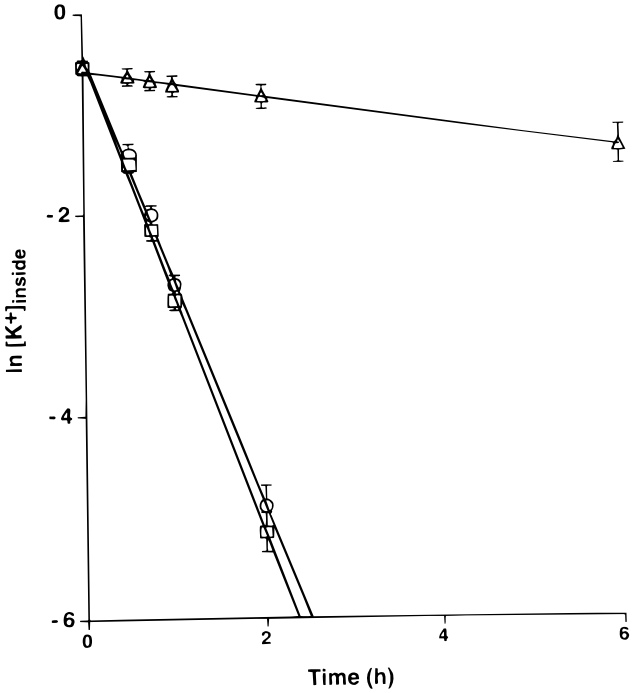

FIGURE 4: Semilog plot of the rate of K^+/Li^+ exchange from the vesicles composed of distinct choline glycerophospholipid subclasses. The concentration of K^+ inside vesicles composed of 16:0-20:4 phosphatidylcholine (□), 16:0-20:4 plasmanylcholine (○), or 16:0-20:4 plasmenylcholine (△) was calculated from the loss of chemical potential in Figure 3 as described in the Materials and Methods. Values shown represent the means ± SD of at least three independent experiments.

these choline glycerophospholipids possessed a similar apparent activation energy for K^+ ion efflux ($E_a = 21 \pm 1$ kcal/mol) but were different in regard to their entropic components (*Y*-intercept) (Figure 8).

The relative entropy of activation of the passive ion permeability in membranes composed of these four phospholipids can be computed as described in the Materials and Methods. With the 16:0-20:4 phosphatidylcholine membrane as a standard (*S′*), the relative entropies of activation for membranes composed of 16:0-20:4 plasmenylcholine, 18:2-18:2 phosphatidylcholine, and 18:1-18:2 phosphatidylcholine were −4.3, −1.3 and −5.9 cal·mol^{-1}·K^{-1}, respectively (Table 3). Similarly, with 16:0-20:4 phosphatidylcholine defined as a standard (*G′*), the relative free energies of activation in membranes composed of 16:0-20:4 plasmenylcholine, 18:2-18:2 phosphatidylcholine, and 18:1-18:2 phosphatidylcholine were calculated to be 1.3, 0.38, and 1.7 kcal/mol, respectively (Table 3). This is consistent with previous results demonstrating that membranes composed of plasmenylcholine are more compact than those of phosphatidylcholine (*32*). The results also suggest that increasing the number of double bonds in the acyl chains results in an increase of packing defects in the membrane facilitating ion passage (see Discussion).

DISCUSSION

Electrically active cells maintain their transmembrane ionic gradients through the precisely orchestrated function of a wide variety of specific ion channels, ion transporters and transmembrane ion pumps. The efficient maintenance of cellular transmembrane ion concentration gradients generated

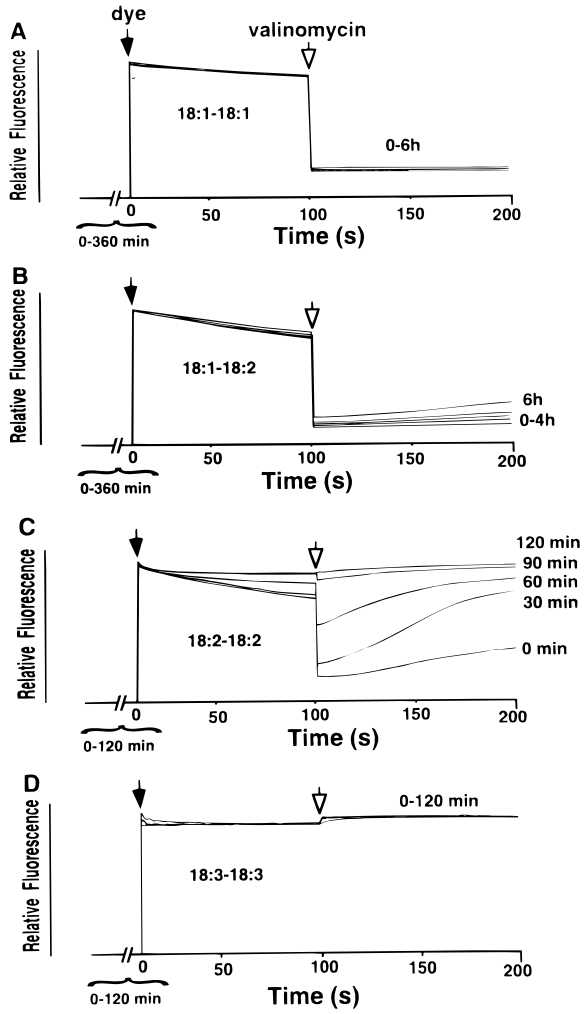

FIGURE 5: Effects of acyl chain unsaturation on the passive ion permeability of vesicle membranes composed of individual phosphatidylcholine molecular species. Small unilamellar vesicles composed of 18:1-18:1 phosphatidylcholine (A), 18:1-18:2 phosphatidylcholine (B), 18:2-18:2 phosphatidylcholine (C), or 18:3-18:3 phosphatidylcholine (D) were prepared in K^+ medium (0.29 M K_2SO_4, pH 6.3 at 22 °C) as described in the Materials and Methods. Vesicles were diluted 100-fold with isoosmotic Li^+ medium (0.29 M Li_2SO_4, pH 6.3 at 22 °C), resulting in a chemical potential across the bilayers. The diluted vesicles were gently stirred at 22 °C for the indicated times prior to the addition of the potential-sensitive fluorescence dye, $diSC_3(5)$ (final concentration, 1×10^{-6} M, dissolved in 4 μL of ethanol). Next, valinomycin (final concentration, 1×10^{-6} M, dissolved in 4 μL of ethanol) was added, and the fluorescence emission was monitored at 690 nm after excitation at 618 nm.

by these protein constituents requires an effective permeability barrier that is provided by the membrane phospholipid bilayer. Despite the known importance of the passive membrane ion permeability properties of the membrane bilayer (*33*−*35*), the role of structural alterations in phospholipid constituents (i.e., alterations in the phospholipid classes, subclasses, and individual molecular species) has not been forthcoming. In this study, we developed a rapid and efficient method for quantifying the passive membrane permeability properties of phospholipid bilayers and have applied this methodology to quantify the first-order rate constant of ion flux utilizing membranes composed of a wide variety of phospholipid classes, subclasses, and individual molecular species. The present results demonstrate that each of the covalent alterations underlying the molecular diversity

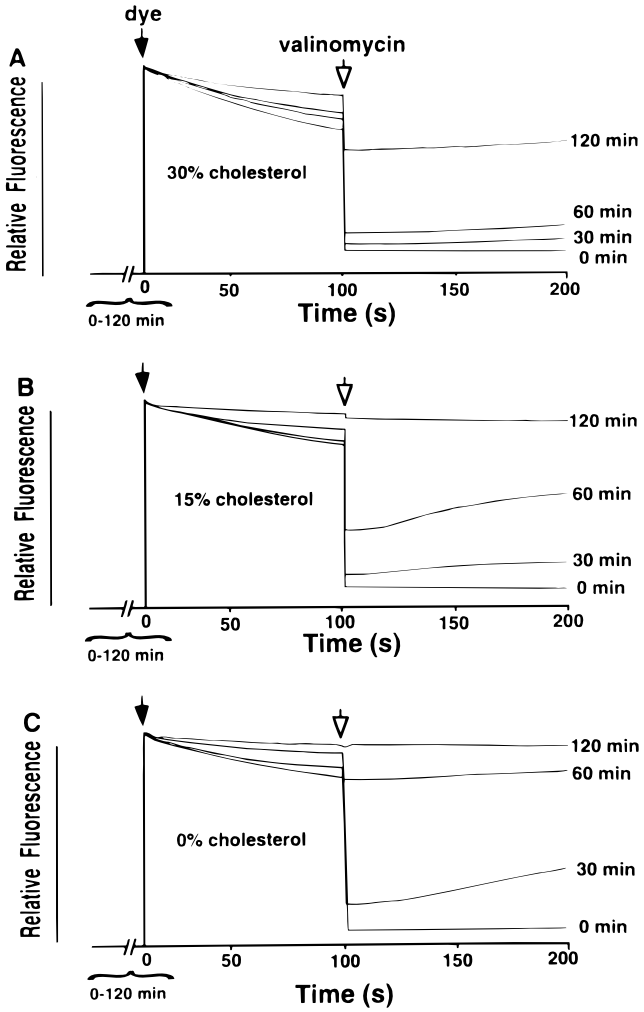

FIGURE 6: Effect of cholesterol on the passive ion permeability of vesicles composed of 16:0-20:4 phosphatidylcholine. Small unilamellar vesicles composed of a binary mixture of phosphatidylcholine containing 30 mol % (A), 15 mol % (B), or 0 mol % (C) cholesterol were prepared in K^+ medium (0.29 M K_2SO_4, pH 6.3 at 22 °C) as described in the Materials and Methods. Vesicles were diluted 100-fold with isoosmotic Li^+ medium (0.29 M Li_2SO_4, pH 6.3 at 22 °C), resulting in a chemical potential across the bilayers, and were gently stirred for 0−120 min at 22 °C. Next, the potential-sensitive fluorescence dye, $diSC_3(5)$ (final concentration, 1×10^{-6} M, dissolved in 4 μL of ethanol) was added prior to the addition of valinomycin (final concentration, 1×10^{-6} M, dissolved in 4 μL of ethanol). Fluorescence emission was monitored at 690 nm after excitation at 618 nm.

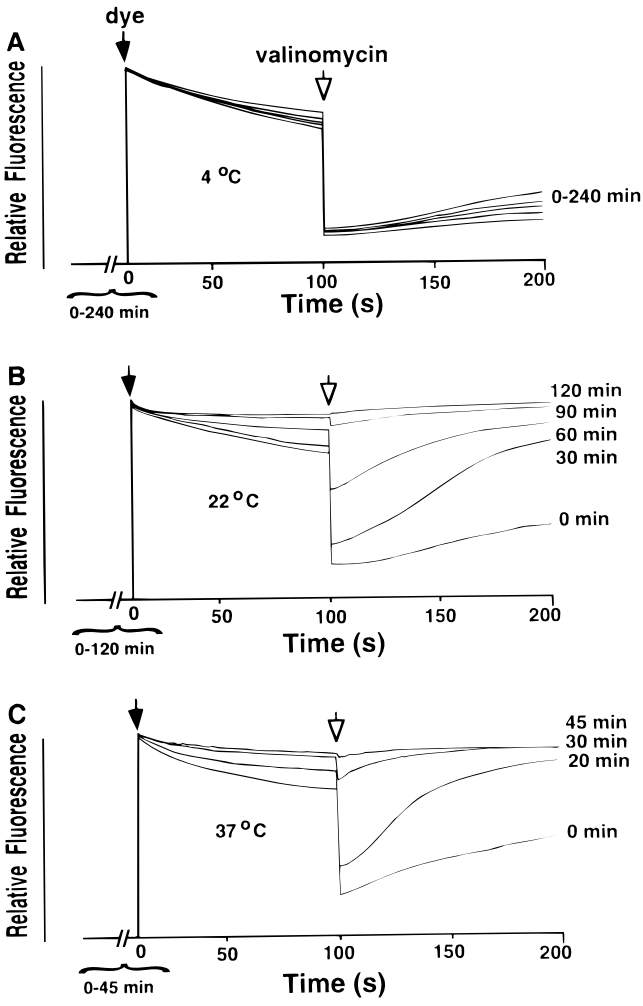

FIGURE 7: Temperature dependence of the passive ion permeability of vesicles composed of 18:2-18:2 phosphatidylcholine. Small unilamellar vesicles composed of 18:2-18:2 phosphatidylcholine, prepared in K^+ medium (0.29 M K_2SO_4, pH 6.3 at 22 °C), were prepared as described in the Materials and Methods. Next, vesicles were diluted 100-fold with isoosmotic Li^+ medium (0.29 M Li_2SO_4, pH 6.3 at 22 °C), resulting in a chemical potential across the bilayers. The diluted vesicles were gently stirred at 4 °C (A), 22 °C (B), or 37 °C (C) for the indicated times. Next, the potential-sensitive fluorescence dye, $diSC_3(5)$ (final concentration, 1×10^{-6} M, dissolved in 4 μL of ethanol) was added prior to the addition of valinomycin (final concentration, 1×10^{-6} M, dissolved in 4 μL of ethanol). Fluorescence emission was monitored at 690 nm with excitation at 618 nm.

of phospholipids present in cellular membranes has important effects on transmembrane passive ion permeability properties.

It has previously been accepted that membranes composed of phosphatidylcholine are effective permeability barriers to the passive movement of ions along their transmembrane ion concentration gradients (*8*). However, the present results demonstrate that only certain specific individual molecular species of phosphatidylcholine are effective barriers. For example, although vesicles composed of 16:0-18:1 phosphatidylcholine did not leak K^+ and Li^+ ions even after incubation at 22 °C for 3 days, vesicles composed of 16:0-20:4 phosphatidylcholine rapidly exchanged K^+ and Li^+ ions along their respective concentration gradients ($k_{app} = 0.04$ min^{-1}). Similarly, other phosphatidylcholine molecular species containing multiple olefin centers (e.g., 18:2-18:2 phosphatidylcholine) also do not provide efficient permeability barriers and allow the rapid passage of K^+ and Li^+ ions ($k_{app} = 0.021$ min^{-1} for 18:2−18:2 phosphatidylcholine).

Lipid-derived signaling pathways in mammalian cells exploit chemical information inherent in the structure of multiple oxidation products of arachidonic acid to communicate biologic information (*36*, *37*). In resting cells, arachidonic acid is stored in the *sn*-2 position of cellular phospholipids and is liberated by the action of one or more phospholipases during cellular activation (*38*, *39*). Since the present results demonstrate that phosphatidylcholine containing arachidonic acid in the *sn*-2 position allows a substantial movement of ions across the membrane, the efficient utilization of cellular energy requires that the arachidonic acid be stored in a chemical moiety which does not promote transmembrane ion flux. Plasmalogens are specialized phospholipids that possess a vinyl ether linkage at the *sn*-1 position and adapt a conformation and dynamic motional

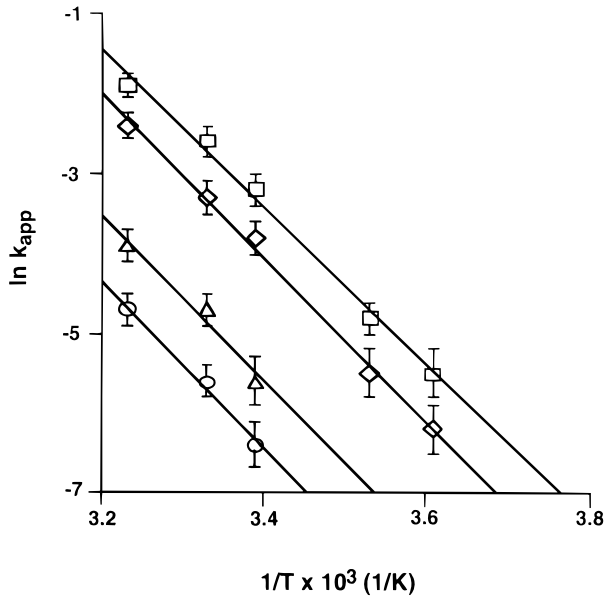

FIGURE 8: Arrhenius plot of the passive ion flux across vesicles composed of distinct choline glycerophospholipid subclasses and molecular species. Passive ion permeability was measured as described in the legend of Figure 7. The rates of K^+/Li^+ exchange from the vesicles composed of 16:0-20:4 phosphatidylcholine (□), 16:0-20:4 plasmenylcholine (◇), 18:2-18:2 phosphatidylcholine (△), or 18:1-18:2 phosphatidylcholine (○) were calculated from the slope of the initial loss of chemical potential as described in the Materials and Methods. Data shown represent the means ± SD of three independent experiments.

regime which is separate and distinct from their diacyl phospholipid counterparts (*26*, *32*, *40*−*43*). The present results demonstrate that plasmalogens containing arachidonic acid at the *sn*-2 position can efficiently store arachidonic acid without an accompanying rapid ion flux along their transmembrane concentration gradients. Accordingly, the present results suggest that one potential reason underlying the predominance of plasmalogens in electrically active membranes is to foster the efficient preservation of transmembrane ion gradients in a cellular membrane that is committed to maintaining high concentrations of arachidonic acid for lipid signal transduction pathways.

Detailed comparisons of transmembrane passive ion flux reveal substantial differences in ion leakage among different phospholipid classes, subclasses, and individual molecular species. Multiple distinct mechanisms probably contribute to the observed differences in transmembrane passive ion flux. These mechanisms include, but are not limited to, alterations in (1) membrane packing (i.e., molecular dynamics), (2) membrane dipoles, and (3) membrane surface charge characteristics. In regard to the first mechanism, one theory of passive membrane ion flux holds that the rate of transmembrane ion flux is dependent upon the dynamic reorganization of packing defects accompanied by the simultaneous movement of ions into these newly created crevices (*44*). The present results show that an increase in the degree of unsaturation in the 18-carbon acyl chain in phosphatidylcholine molecular species results in a dramatic increase in the passive ion permeability. Moreover, cholesterol, which increases the density and decreases the fluidity of membrane (*31*, *42*, *45*, *46*), greatly inhibits the passive ion permeability of the membrane. These effects are anticipated to contribute to alterations in the entropic component modulating transmembrane ion flux, and the results of the Arrhenius analyses are consistent with this possibility. In regard to the second mechanism, the importance of membrane dipoles in organizing membrane surface charge and in modulating transmembrane ion flux has previously been recognized (*5*, *6*). The present results demonstrate dramatic differences in passive ion permeability properties of vesicles composed of plasmenylcholine and phosphatidylcholine which are not reflected in their apparent activation energies for ion flux. Thus, the differences in the surface dipole moment of membranes composed of phosphatidylcholine and plasmanylcholine do not seem to be responsible for the majority of the observed alterations. However, we point out the importance of surface dipoles cannot be definitively excluded due to the possibility that membranes composed of each phospholipid subclass also possess distinct probability factors (A) in the Arrhenius equation, which we had assumed to be identical. Previous work has demonstrated that the molecular conformation and dynamics of vesicles composed of plasmalogens are substantially different from vesicles composed of alkyl ether or diacyl glycerophospholipids (*32*, *40*, *43*, *47*). The present results suggest that these conformational and dynamic considerations are important in the observed subclass differences for passive ion flux. Finally, in regard to the third mechanism, the importance of membrane surface charge is manifest as an increase in the restraining force of cations in negatively charged phosphatidylserine membrane matrixes. Thus, this component could manifest itself in the frequency of productive interactions of ions with the membrane interface.

In conclusion, the present results underscore the importance of apparently modest covalent alterations in phospholipid structure as important determinants of the rate of passive ion permeability. Moreover, the results identify the importance of structure-induced packing defects in the membrane bilayer as a modulator of passive ion permeability. The observed difference in passive ion permeability properties of plasmalogens and diacyl phospholipids could contribute to the predominance of plasmalogens in electrically active tissues.

REFERENCES

1. Singer, S. J. and Nicholson, G. L. (1972) *Science 175*, 720−731.
2. Cullis, P. R. and de Kruijff, B. (1979) *Biochim. Biophys. Acta 559*, 399−420.
3. Kim, D. and Clapham, D. E. (1989) *Science 244*, 1174−1176.
4. Chen, X. and Gross, R. W. (1995) *Biochemistry 34*, 7356−7364.
5. Chen, X. and Gross, R. W. (1994) *Biochemistry 33*, 13769−13774.
6. Flewelling, R. L. and Hubbell, W. L. (1986) *Biophys. J. 49*, 541−552.
7. Seelig, J., Macdonald P. M., and Scherer, P. G. (1987) *Biochemistry 26*, 7535−7542.
8. Cullis, P. R. and Hope, M. J. (1991) in *Biochemistry of Lipids, Lipoproteins and Membranes*, (Vance, D. E., and Vance, J., Eds.) pp 1−41, Vol. 20, Elsevier Science Publishers, Amsterdam, The Netherlands.
9. Dowhan, W. (1997) *Annu. Rev. Biochem. 66*, 199−232.
10. Boggs, J. M., Stamp, D., Hughes, D. W., and Deber, C. M. (1981) *Biochemistry 20*, 5728−5735.
11. Buldt, G. and Wohlgemuth, R. (1981) *J. Membr. Biol. 58*, 81−100.

12. Stubbs, C. D. and Smith, A. D. (1984) *Biochim. Biophys. Acta 779*, 89−137.
13. Yeagle, P. L. (1989) *FASEB J. 3*, 1833−1842.
14. Gross, R. W. (1984) *Biochemistry 23*, 158−165.
15. Gross, R. W. (1985) *Biochemistry 24*, 1662−1668.
16. Ford, D. and Gross, R. W. (1989) *Proc. Natl. Acad. Sci. U.S.A. 86*, 3479−3483.
17. Moolenaar, W. H. and Spector, I. (1977) *Science 196*, 331−333.
18. Hermetter, A. and Paltauf, F. (1981) *Chem. Phys. Lipids 29*, 225−233.
19. Elinder F. and Arhem P. (1991). *Neuroreport 2*, 685−687.
20. Birnir, B., Tierney, M. L., Howitt, S. M., Cox, G. B., and Gage, P. W. (1992) *Proc. R. Soc. Lond. B. 250*, 307−312.
21. Piguet, P. and North R. A. (1992) *J. Cell. Phys. 151*, 269−275.
22. Han, X., Zupan, L. A., Hazen, S. L. and Gross, R. W. (1992) *Anal. Biochem. 200*, 119−124.
23. Bligh, E. G. and Dyer, W. J. (1959) *Can. J. Biochem. Physiol. 37*, 911−917.
24. Fink, L. W. and Gross, R. W. (1984) *Circ. Res. 55*, 585−94.
25. Kolchens, S., Ramaswami, V., Birgenheier, J., Nett, L., and O'Brien, D. F. (1993) *Chem. Phys. Lipids 65*, 1−10.
26. Chen, X., Han, X., and Gross, R. W. (1993) *Biochim. Biophys. Acta 1149*, 241−248.
27. Waggoner, A. (1976) *J. Membr. Biol. 27*, 317−334.
28. Szabo, G. (1974) *Nature 252*, 47−49.
29. Jain, M. K., Singer, M. A., Ramirez, F., Marecek, J. F., He, N. B., and Hui, S. W. (1984) *Biochim. Biophys. Acta 775*, 426−434.
30. Semple, S. C., Chonn, A., and Cullis, P. R. (1996) *Biochemistry 35*, 2521−2525.
31. Stillwell, W., Dallman, T., Dumaual, A. C., Crump, F. T., and Jenski, L. J. (1996) *Biochemistry 35*, 13353−13362.
32. Han, X. and Gross, R. W. (1990) *Biochemistry 29*, 4992−4996.
33. Cruzeiro-Hansson, L. and Mouritsen, O. G. (1988) *Biochim. Biophys. Acta 944*, 63−72.
34. Corvera, E., Mouritsen, O. G., Singer, M. A., and Zuckermann, M. J. (1992) *Biochim. Biophys. Acta 1107*, 261−270.
35. Fyles, T. M., James, T. D., and Kaye, K. C. (1993) *J. Am. Chem. Soc. 115*, 12315−12321.
36. Smith, W. L. (1989) *Biochem. J. 259*, 315−324.
37. Janssen-Timmen, U., Tomic, I., Specht, E., Beilecke, U., and Habenicht, A. J. (1994) *Ann. N. Y. Acad. Sci. 733*, 325−334.
38. Dennis, E. A. (1987) *Biotechnology 5*, 1294−1300.
39. Gross, R. W. (1995) *J. Lipid Mediators Cell Signaling 12*, 131−137.
40. Pak, J. H., Bork, V. P., Norberg, R. E., Creer, M. H., Wolf, R. A., and Gross, R. W. (1987) *Biochemistry 26*, 4824−4830.
41. Han, X. and Gross, R. W. (1991) *Biochim. Biophys. Acta 1069*, 37−45.
42. Han, X. and Gross, R. W. (1991) *Biochim. Biophys. Acta 1063*, 129−136.
43. Han, X., Chen, X., and Gross, R. W. (1991) *J. Am. Chem. Soc. 113*, 7104−7109.
44. Träuble, H. (1971) *J. Membr. Biol. 4*, 193−208.
45. Yeagle, P. L. (1987) *The Membranes of Cells*, pp 120−140, Academic Press, New York.
46. McMullen, T. P., Lewis, R. N. A. H., and McElhaney, R. N. (1994) *Biophys. J. 66*, 741−752.
47. Malthaner, M., Hermetter, A., Paltauf, F., and Seelig, J. (1987) *Biochim. Biophys. Acta 900*, 191−197.

BI9725172